Developmental Cell
Article

Drosophila HOPS and AP-3 Complex Genes Are Required for a Deltex-Regulated Activation of Notch in the Endosomal Trafficking Pathway

Marian Wilkin,[1] Pajaree Tongngok,[1] Nicole Gensch,[1] Sylvaine Clemence,[1] Masato Motoki,[1] Kenta Yamada,[2] Kazuya Hori,[2] Maiko Taniguchi-Kanai,[2] Emily Franklin,[1] Kenji Matsuno,[2] and Martin Baron[1,*]
[1]Faculty of Life Sciences, University of Manchester, Michael Smith Building, Oxford Road, Manchester, M13 9PT, UK
[2]Department of Biological Science and Technology, Tokyo University of Science, 2641 Yamazaki, Noda, Chiba, 278-8510 Japan
*Correspondence: mbaron@manchester.ac.uk
DOI 10.1016/j.devcel.2008.09.002

SUMMARY

DSL ligands promote proteolysis of the Notch receptor, to release active Notch intracellular domain (N^{ICD}). Conversely, the E3 ubiquitin ligase Deltex can activate ligand-independent Notch proteolysis and signaling. Here we show that Deltex effects require endocytic trafficking by HOPS and AP-3 complexes. Our data suggest that Deltex shunts Notch into an endocytic pathway with two possible endpoints. If Notch transits into the lysosome lumen, it is degraded. However, if HOPS and AP-3 deliver Notch to the limiting membrane of the lysosome, degradation of the Notch extracellular domain allows subsequent Presenilin-mediated release of N^{ICD}. This model accounts for positive and negative regulatory effects of Deltex in vivo. Indeed, we uncover HOPS/AP-3 contributions to Notch signaling during *Drosophila* midline formation and neurogenesis. We discuss ways in which these endocytic pathways may modulate ligand-dependent and -independent events, as a mechanism that can potentiate Notch signaling or dampen noise in the signaling network.

INTRODUCTION

The Notch receptor mediates a cell-cell signal, which is utilized repeatedly to regulate pattern formation and cell fate during development (Lai, 2004). Ectopic activation of Notch is involved in several cancers including melanoma, T cell acute lymphoblastic leukemia (T-ALL), and cancers of the breast, lung, and ovary (Roy et al., 2007). Understanding different mechanisms of Notch activation and misactivation will be important for developing therapeutic strategies to interfere with Notch function in these conditions. Notch is a transmembrane receptor protein that is activated by DSL (Delta/Serrate/Lag-2)-domain ligands (Baron, 2003). Ligand binding initiates proteolytic cleavages that first remove the majority of the Notch extracellular domain through the activity of an ADAM metalloprotease enzyme (ectodomain shedding), and then release the soluble intracellular domain by an intramembrane cleavage. This regulated intramembrane cleavage (RIP) depends on the γ-secretase complex, which includes the aspartate protease Presenilin (Psn). The Notch intracellular domain is then targeted to the nucleus where it interacts with a CSL (CBF1/Suppressor of Hairless/Lag-2)-transcription factor to activate expression of Notch target genes.

Ligand-dependent activation of Notch is thought to occur at the cell surface. However, we have shown previously that the overexpression of Deltex (Dx), an intracellular Notch-binding ring finger E3 ubiquitin ligase, bypasses the requirement for DSL-ligands and promotes Notch activation by a poorly characterized, but endocytic-dependent, mechanism (Hori et al., 2004). We have also shown that sorting of Notch within the early endosome, between different compartments, is associated with activation or downregulation of Notch (Wilkin et al., 2004). Furthermore, loss of function of several endosomal membrane trafficking components including *TSG101*, *Vps25*, and *Lethal giant discs* (Moberg et al., 2005; Thompson et al., 2005; Vaccari and Bilder, 2005; Jaekel and Klein, 2006) results in ectopic Notch activation in an undefined endocytic compartment. How Notch is subsequently activated by this route, the location in the cell where this occurs, and the relationship of this mechanism to the canonical pathway is not known. Here we used a phenotypic screen based on ectopic Dx expression in the *Drosophila* wing imaginal disc, to identify genes that are required for endocytic-Notch activation. We show that Dx-induced signaling depends on the activity of several members of the HOPS (homotypic fusion and vacuole protein sorting) and AP-3 (Adaptor protein-3) complexes and is promoted by Rab7, a GTPase that is involved in trafficking to the late endosome and fusion to the lysosome. We further show that mutations of *dx*, AP-3, or HOPS complex genes reduce Notch signaling during *Drosophila* embryonic development. We propose a model whereby Dx-induced delivery of Notch to the limiting membrane of the late endosome/lysosome results in Notch ectodomain shedding and Notch activation in a Psn-dependent manner.

RESULTS

Dx-Regulated Notch Signaling Requires Components of the HOPS and AP-3 Complexes

Overexpression of Dx strongly depletes Notch from the adherens junction, and induces the activation of Notch signaling in an endocytic-dependent but Delta/Serrate-independent manner (Hori et al., 2004, Figures 1A and 1B). Rab5 is a small GTPase that orchestrates trafficking through the early endosome (Pfeffer, 2003). Coexpression of Dx with Rab5 GTPase blocked ectopic

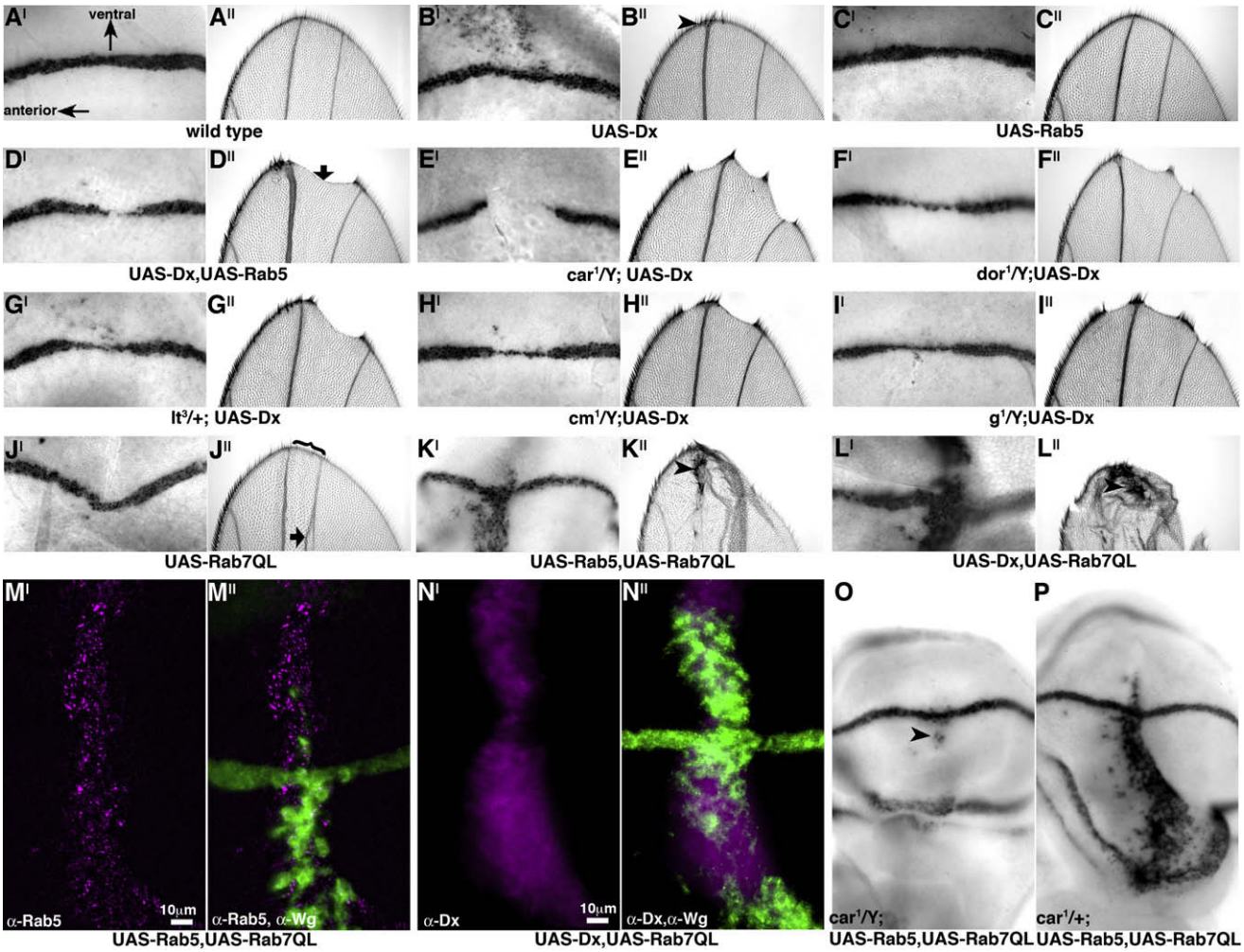

Figure 1. Early and Late Endocytic Trafficking Components Alter the Outcome of Dx Overexpression

(A–L; O–P) *wg RNA* expression in 3rd instar larval wing discs and adult wing tips.

(A) Wild-type.

(B) Dx overexpression (arrowhead marks ectopic margin, [B″]).

(C) Rab5 overexpression.

(D) Rab5 and Dx coexpression. Arrow marks margin notching (arrow, [D″]).

(E–I) Similar results were obtained when Dx was overexpressed in mutant backgrounds for: (E) car^1, (F) dor^1; (G) lt^3/+; (H) cm^1; and (I) g^1.

(J) Overexpression of Rab7QL distorts the D/V boundary (J′), narrows the region bracketed in (J″), and causes abnormal vein trajectories (arrow, [J″]), but does not affect Notch signaling.

(K and L) Rab7QL coexpressed with either Rab5 (K), or Dx (L) results in strong ectopic *wg*, and extra wing margin (arrowheads [K″], and [L″]).

(M and N) Notch activation, marked with anti-Wg (green), occurs within cells coexpressing Rab5 (purple) and Rab7QL (M), or Dx (purple) and Rab7QL (N) (ten sequential optical sections merged).

(O and P) Overexpression of Rab5 and Rab7QL in (O) hemizygous car^1/γ (arrowhead, suppressed ectopic *wg*) or (P) in a car^1/+ background.

Dx-induced Notch signaling and inhibited endogenous Notch activity, whereas Rab5 GTPase expression alone had no effect on Notch activity (Figures 1C and 1D). Despite this, overexpression of Rab5 forced accumulation of Notch in enlarged Rab5-positive endosomal structures (Figure 2A). Interestingly, overexpression of Rab5 did not deplete Notch from the adherens junction to the same extent as Dx (see Figure S1 available online). This suggests that a pool of adherens junction Notch is insensitive to Rab5 activity, or that recycling of Notch from the Rab5-sensitive pool maintained a steady-state level of adherens junction Notch. Our working model to explain these data is that there are two mechanisms by which Notch can be activated. In this model, Dx activity may transfer full-length Notch from a pool that is competent for ligand-dependent activation. Endocytic Notch activation may then occur by a separate mechanism thus compensating for the loss of the signal due to the depletion of the cell surface pool. However if progression of endocytosed Notch to an activating compartment was blocked, then no ectopic activation would occur and the loss of Notch signal from the cell surface pool would be evident. Providing an excess of Rab5 may be one way of blocking the onward trafficking of Notch, by sequestering factors necessary for late endosomal

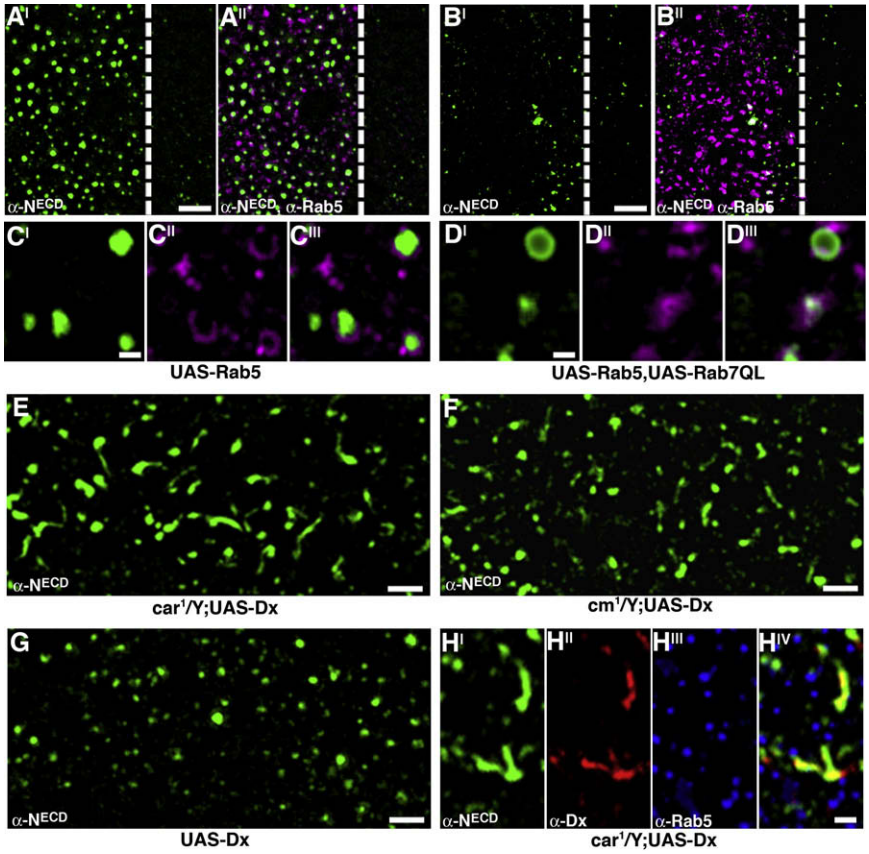

Figure 2. Regulation of Notch Progression through the Endosomal Pathway

(A–D) Location of endogenous Notch (green) when Rab5 (purple) is overexpressed (A) and (C) or Rab5 is coexpressed with Rab7QL (B and D).

(E–G) Overexpression of Dx in (E) *car*^{1}, or (F) *cm*^{1}, but not in (G) wild-type, results in the accumulation of Notch (anti-N^{ECD}, green) in tubular structures.

(H) The tubular Notch (green) that accumulates when Dx is overexpressed in a *car*^{1} background is colocalized with Dx (anti-Dx, red), and emanates basally into the cell from the location of the Rab5 compartment (anti-Rab5, blue).

(A), (B), and (E–H) display merged stacks of four optical sections, 1.5 μm–3 μm below the adherens junction. In (C and D) an optical section 2.5 μm below the adherens junction is shown. Scale bars: (A and B) = 10 μm; (E–G) = 5 μm; (C), (D), and (H) = 1 μm. Overexpression was carried out using the Dpp-Gal4 driver.

maturation (Rink et al., 2005). Considerable Notch accumulation in Rab5 positive vesicles occurred when Dx was coexpressed with Rab5 (Figure S1).

We used the above-described phenotypic switch between Dx-induced Notch activation and downregulation as a basis to identify genes whose wild-type function is required for Dx-dependent Notch signaling. We found that mutations in several genes involved in *Drosophila* eye pigmentation, *light* (*lt*), *carnation* (*car*), *deep orange* (*dor*), *garnet* (*g*), *carmine* (*cm*), and *ruby* (*rb*) were capable of converting the results of Dx overexpression from a gain of function to a loss of function of Notch activity (Figures 1E–1I; Table S1). The proteins encoded by these genes are respectively *Drosophila* homologs of the HOPS complex components (VPS41, VPS33A, VPS18) which mediate late endosomal maturation and lysosomal fusion (Warner et al., 1998; Seals et al., 2000; Wurmser et al., 2000; Rink et al., 2005), and the Adaptor Protein-3 (AP-3) complex components (δ, μ3A, β3A) which traffic proteins to the lysosomal limiting membrane (Peden et al., 2004; Theos et al., 2005). To investigate whether HOPS and AP-3 complex genes affected Dx-induced Notch endocytosis, we investigated the localization of Notch in the background of mutations in *car* and *cm*. Notch was accumulated in long tubular structures, associated with Dx, and emanating from the plane of Rab5 marked early endosomes, which were not observed when Dx was expressed in a wild-type background (Figures 2E–2H).

Because Dx-induced Notch trafficking appeared to be retarded in an early endosome compartment by *car* and *cm* mutations, we tested if accelerating early to late endosomal trafficking resulted in Notch signal activation. During endosomal maturation from early to late endosomes, Rab5 is replaced on the endosomal membrane by another small GTPase, Rab7 (Rink et al., 2005). The latter regulates late endosomal trafficking and fusion to the lysosomes (Bucci et al., 2000). We expressed Rab7QL, which is a constitutively active form of the Rab7 GTPase that accelerates late endosomal trafficking and lysosomal fusion (Entchev et al., 2000; Bucci et al., 2000; Seals et al., 2000). No increase in Notch signaling was evident with Rab7QL expression alone (Figure 1J). However if Rab5 was coexpressed, then Notch signaling was activated cell-autonomously, in a *car*-dependent manner (Figures 1K, 1M, 1O, and 1P). Notch was no longer strongly accumulated within large Rab5 positive vesicles, but was sometimes located in ring-like structures adjacent to Rab5 staining (Figures 2A–2D). These data suggest that Rab7QL may overcome the sequestration by Rab5 of factors, such as HOPS complex components, which would normally be required for Rab5/Rab7 endosomal conversion and maturation of early to late endosomes (Rink et al., 2005). Dx was able to substitute for Rab5 overexpression and synergistically promoted strong cell-autonomous Notch signal activation by Rab7QL (Figures 1L and 1N), presumably by ensuring a sufficient pool of endosomal Notch.

Rab7-dependent late endosomal trafficking therefore enables the endocytic pool of Notch to reach a location where it is available for activation. Interestingly, although *car*^{1} suppressed the Notch signaling that resulted from Rab5/Rab7QL coexpression, it did not suppress endogenous Notch D/V boundary signaling (Figures 1O and 1P). This is probably because, unlike Dx, Rab5/Rab7QL does not deplete the ligand-sensitive pool and only activates a Rab5-sensitive pool. We also found that *car*^{1} and *rb*^{1} did not suppress ligand-dependent activation of Notch (Figure S2), consistent with the presence of two distinct mechanisms of Notch activation.

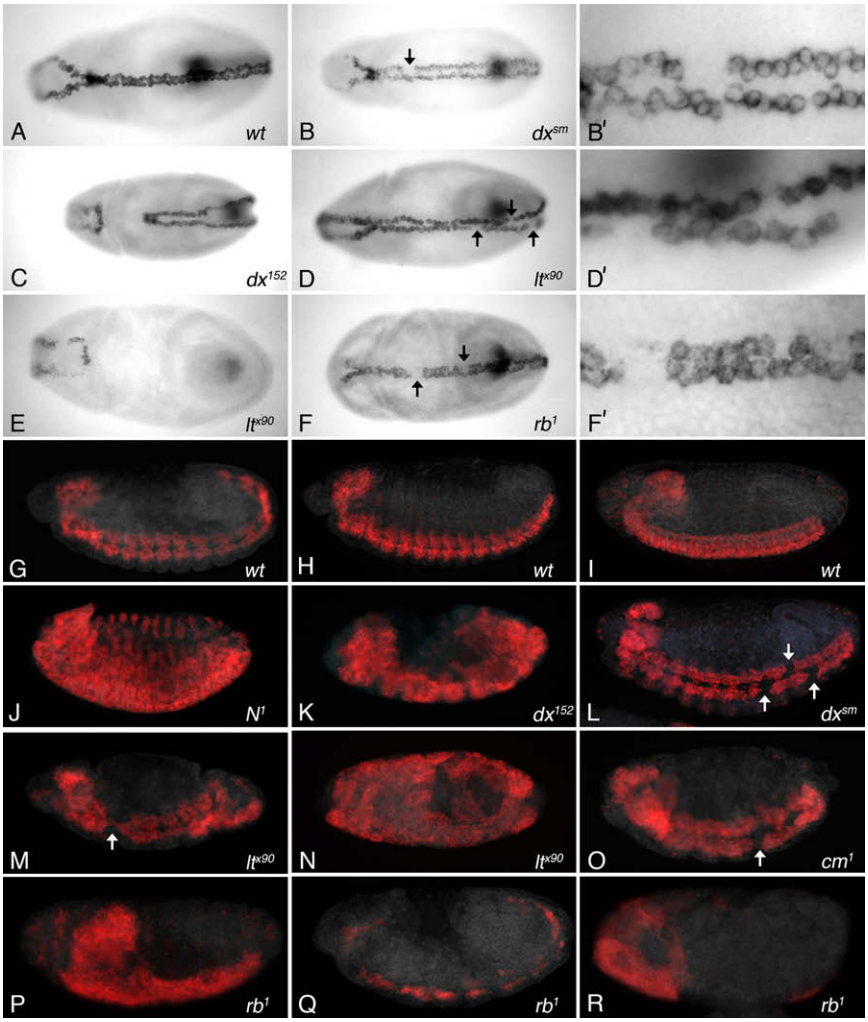

Figure 3. Embryonic Phenotypes Resulting from *dx*, *HOPS*, or *AP-3* Gene Mutants

(A–F) *sim* mRNA expression in stage 8 embryos.

(A) Wild-type.

(B–F) Examples of mild to severe loss of *sim* expression in *dx*, *lt*, and *rb* mutant embryos.

(B′), (D′), and (F′) Enlargements of regions marked by arrows in (B), (D), and (F).

(G–R) Anti-Elav staining to show the CNS scored in stage 12–16 embryos. Arrows mark loss of nervous system.

(G–I) Wild-type embryos of stage 12, 13, and 15, respectively.

(J) N^1 mutant displaying strong neurogenic phenotype.

(K) dx^{152} embryo with moderate neurogenic phenotype.

(L) dx^{sm} embryo with gaps in CNS.

(M and N) lt^{x90} embryos. (M) Gain and loss of CNS. (N) Strong neurogenic phenotype.

(O) cm^1 embryo with moderate neurogenic phenotype and incomplete ventral nerve cord (VNC).

(P, Q, and R) rb^1 embryos. (P) Moderate neurogenic phenotype. (Q) Gaps in the CNS. (R) Mixed phenotype, with brain expansion but severe loss of VNC staining.

HOPS and AP-3 Complex Components Contribute to Endogenous Notch Signaling

We examined the effect of loss-of-function mutations of HOPS and AP-3 components in a N^{55e11}/+ background. The HOPS complex gene mutations *car* and *lt*, and AP-3 complex gene mutations *cm* and *ruby*, enhanced the penetrance and severity of the wing notching phenotype of adult wings, (N^{55e11}/+ = 5.8% wings with notches, n = 86; N^{55e11}/car^1 = 96.5%, n = 85; N^{55e11}/+; lt^3/+ = 100%, n = 54; N^{55e11}/cm^1 = 89.5%, n = 209; N^{55e11}/rb^1 = 93.1%, n = 102) and reduced the expression of the Notch signal reporter *wg* (Figures S3A–S3F). The wing and leg joint phenotypes of dx^{24} and the wing phenotypes of the hypomorphic Notch mutation, nd^1, were also enhanced by car^1 and lt^3 mutations (Figures S3G–S3P). These data show that, as well as mediating ectopic Dx-induced Notch signaling, the HOPS and AP-3 complexes can contribute to the robustness of full endogenous Notch signaling levels during development. We did not however observe wing margin phenotypes for viable homozygotes *of* car^1, cm^1, rb^1, or lt^{x90}.

Because different tissues may show different sensitivity to reduction of endocytic Notch trafficking, we investigated whether *dx*, HOPS, and AP-3 mutations displayed phenotypes during embryonic development. We used *Drosophila* midline formation and neurogenesis as assays of Notch signaling. Stage 7–10 embryos, grown at 25°C, were stained for *single minded* (*sim*) expression, which is a direct reporter of Notch signal activity (Morel and Schweisguth, 2000). We found that dx^{152}, dx^{sm}, lt^{x90}, and rb^1 showed gaps in *sim* expression with a penetrance of between 13% to 34%, compared with 3.0% for wild-type ($p < 0.05$; Figure 3 and Table 1). When the developing nervous system of stage 12–16 embryos was examined by anti-Elav staining, we found a neurogenic phenotype in dx^{152}, dx^{sm}, lt^{x90}, cm^1, and rb^1 embryos of between 3.4% to 12.6% penetrance, compared to 0.35% for wild-type ($p < 0.05$; Figure 3 and Table 1). Both *sim* expression and neurogenic phenotypes were found to be temperature-sensitive, with penetrance increasing with temperature. For example, at 29°C, cm^1 also produced significant gaps in *sim* expression ($p < 0.05$), while not being significantly different from wild-type at 18 or 25°C. In all mutants, in addition to neurogenic phenotypes, we also observed gaps in the central nervous system, which might reflect either a loss of neurons and/or a failure of neurogenesis. Often a mixture of these phenotypes occurred in individual embryos (Figure 3), and the proportion with this mixed phenotype increased when embryos were developing at 29°C.

Dx Activity Opposes Trafficking of Notch to the Internal Compartments of the Rab7-Positive Late Endosome

We coexpressed Dx with Rab7GFP to investigate the trafficking destination of Notch. Rab7GFP marks the limiting membrane of late endosomes/lysosomes (Bucci et al., 2000), as illustrated by

Table 1. Reduction of Midline *sim* Expression and Neurogenic Phenotypes of *dx*, HOPS, and AP3 Gene Mutants

	Percentage of Embryos Displaying Reduction of *sim* Expression[a]			Percentage of Embryos Displaying Neurogenic[b] Phenotypes		
Genotype	18°C	25°C	29°C	18°C	25°C	29°C
OreR	0.0	3.0	2.4	0.3	0.35	5.6
	n = 113	n = 166	n = 255	n = 346	n = 288[c]	n = 108
dx^{152}	1.6	13.8	24.6	3.4	7.7	18.2
	n = 61	n = 58	n = 167	n = 146	n = 247	n = 126[c]
dx^{sm}	11.9	22.2	49.2	3.8	8.6	35.1
	n = 134	n = 117	n = 63	n = 400	n = 559	n = 74[c]
lt^{x90}	4.6	34.5	43.9	2.5	12.2	60.5
	n = 65	n = 119	n = 107	n = 163	n = 115	n = 43[c]
rb^{1}	1.7	20.5	52.6	2.2	12.6	87.4
	n = 115	n = 44	n = 38	n = 315	n = 247	n = 119[c]
cm^{1}	0.8	3.1	18.9	1.6	3.4	9.4
	n = 125	n = 192	n = 37	n = 184	n = 117	n = 106[c]

$P < 0.05$ for all differences in values compared to OreR at the same temperature (χ^2 test) (except for cm^1 at 18°C and 25°C [*sim* expression] and 29°C [neurogenic phenotype]).

$P < 0.05$ for all differences in values obtained at 29°C compared to the same genotype at 18°C (apart from OreR for *sim* expression).

[a] Defined as the percentage of embryos displaying at least one significant gap in the midline *sim* expression pattern in stage 7–10 embryos.

[b] Neurogenic phenotypes scored as moderate or severe expansion of regions of the embryonic CNS, or mixed phenotypes which included both expansion of some regions of the CNS accompanied by loss or reduction of other regions.

[c] >70% of the scored neurogenic embryos were of the mixed class.

the observation that the Rab7GFP positive vesicles were often associated with the lysosomal marker Arl8 (Hofmann and Munro, 2006) and could be labeled with lysotracker (Figure S4). We found that Notch signaling was still activated by Dx overexpression when Rab7GFP was coexpressed (Figure S4), and basal Rab7-associated Notch was mostly found on the edge of Rab7 positive rings (Figure 4B, 67.3% vesicles with Notch on outer ring, n = 217). In contrast, without Dx overexpression, the Rab7-associated Notch was almost always localized within an internal late endosome compartment, surrounded by rings of Rab7GFP (Figure 4A, 3.2% vesicles with Notch on outer ring, n = 126). Similar observations were made when we stained for either N^{ECD} or N^{ICD} suggesting that full-length Notch could access the late endosome (Figure S5).

We have shown previously that Suppressor of deltex (Su(dx)), an E3 ubiquitin ligase, can downregulate Notch through altering its endosomal sorting (Wilkin et al., 2004). The phenotypic consequences of overexpression of Su(dx) on Dx-induced Notch signaling were similar to the effect of mutations in HOPS and AP-3 complexes, i.e., coexpression of Su(dx) not only blocked ectopic Notch signaling but also cooperated with Dx to downregulate the endogenous D/V boundary Notch activity (Figures 4E–4G). This observation implies that Su(dx) expression blocks the progression of endocytosed Notch to the cell location where it can be activated. However, Su(dx) expression did not block the ability of Dx to induce depletion of Notch from the adherens junctions (Figures 4C and 4H) or prevent onward trafficking from the early endosome (Figures 4D and 4I). Instead Su(dx) reduced Dx/Notch endosomal colocalization (Figures 4D and 4I), and overcame the ability of Dx to promote retention of Notch on the limiting membrane of the late endosome (Figure 4J, 11.3% vesicles with Notch on outer ring, n = 283). Thus the blockage of the Dx-induced signal was correlated with transfer of Notch into the internal compartment of the late endosome.

We considered whether the use of Rab7GFP expression, which enlarges the late endosomal compartment, was driving Notch into a physiologically irrelevant location. We therefore utilized an alternative method, i.e., by marking the late endosome limiting membrane with anti-ubiquitin. In the late endosome, ubiquitin is restricted to the limiting membrane because when ubiquitinated proteins are transferred into the internal compartments of the multivesicular body they are deubiquitinated (Dupre and Haguenauer-Tsapis, 2001). When endocytic Notch signaling was activated by coexpression of Notch with $Su(dx)^{\Delta HECT}$, a dominant negative form of Su(dx) (Wilkin et al., 2004), we found Notch localized in rings, colocalized with ubiquitin in vesicular structures around 3 μm below the plane of the adherens junctions. In contrast, when full-length Su(dx) was expressed, late endosomal Notch was localized in the center of the ubiquitin marked structures (Figure S6). Thus a similar correlation between signaling and delayed transfer from the late endosomal limiting membrane was evident when late endosomes were not perturbed by Rab7 overexpression.

Dx Promotes Ectodomain Shedding and Vesicular Accumulation of Notch Intracellular Domain

To investigate if Notch ectodomain shedding occurred in response to Dx activity we utilized a C-terminally YFP-tagged Notch and scored the frequency of vesicles containing extra- and intracellular Notch epitopes. The N^{YFP} construct responded to the coexpression of Dx by strongly activating Notch signaling (Figures 5A–5C). When the distribution of the Notch-YFP tag was compared to the N^{ICD} epitope, a near complete codistribution was observed (Figure 5E), showing that the tag was not significantly cleaved from the Notch intracellular domain. In contrast, when costained with anti-N^{ECD}, only 60%–80% of Notch containing vesicles contained both N^{ECD} and YFP epitopes (Figures 5D, 5F, and 5G). This was the case whether Dx was coexpressed or

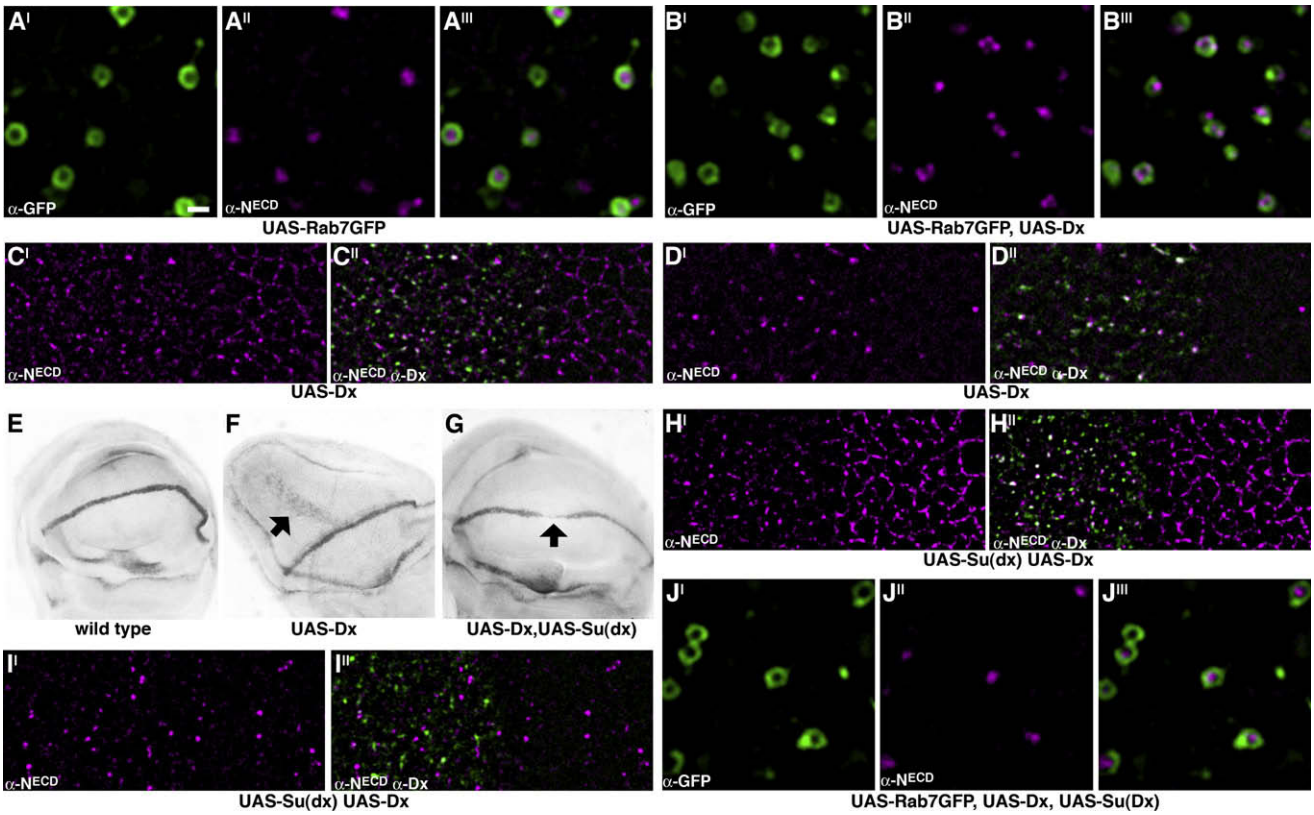

Figure 4. Dx-Induced Notch Activation Is Associated with Retention of Notch at the Limiting Membrane of the Late Endosome

(A and B) Localization of basal Notch (anti-N^{ECD}, purple) compared with Rab7GFP (green) following expression of (A) Rab7GFP and (B) Dx and Rab7GFP.

(C and D) Overexpression of Dx (green) depletes Notch (anti-N^{ECD}, purple) from the adherens junctions (C). Residual junctional Notch partially colocalizes with Dx, as does (D) the Notch within early endosomes located 1.5 μm more basal.

(E–G) *wg* mRNA expression. (E) Wild-type. (F) Dx overexpression causing ectopic *wg* (arrow).

(G–J) Coexpression of Su(dx) and Dx. (G) There is no ectopic *wg* and endogenous *wg* is reduced (arrow). (H) Endogenous Notch (purple) is depleted from the adherens junctions. (I) One and a half micrometers more basal, Notch is in spherical vesicles, but less accumulated than when Dx is expressed alone, and does not colocalize with Dx. (J) the majority of the basal Notch is in the middle of a Rab7GFP ring. Scale bar: (A, B, and J) = 1 μm; (C, D, H, and I) = 2 μm. Overexpression was performed using Dpp-Gal4 (A–B, and J) or Ptc-GAL4 (C–I).

not and suggested that there is a basal level of ectodomain shedding which is not associated with signal-upregulation. Dx expression did affect the relative proportion of YFP-only and N^{ECD}-only vesicles (Figures 5F and 5G). When Dx was not overexpressed, the relative frequency of YFP-only and N^{ECD}-only vesicles did not differ significantly from a 1:1 ratio when scored at different planes within the cell along the apical-basal axis.

In contrast, when Dx was overexpressed, we consistently observed an accumulation of YFP-only vesicles relative to N^{ECD}-only vesicles at 3 μm below the plane of the adherens junctions ($p = 0.03$), but not at other planes. The latter may be explained if Dx-induced Notch ectodomain shedding was accompanied by degradation of the N^{ECD} in the late endosomal pathway. Consistent with the above data, we found that Dx expression caused an accumulation of Notch fragments, which migrated around 120–140kD, and stained with anti-N^{ICD} on western blots (Figure 5H). The accumulation of the Dx-induced fragments was prevented by coexpression with Su(dx) (Figure 5H), correlating with the downregulation of Dx-induced signaling. We utilized a TAP-tag/TEV protease affinity purification to purify overexpressed N^{TAP} (Veraksa et al., 2005) from wing discs, and showed that when Dx was expressed the accumulated truncated Notch fragments were ubiquitinated (Figure 5I). We also found that Dx-induced Notch signaling was dependent on the activity of Psn (Figure 6). Since Psn acts on membrane-tethered substrates with short extracellular domains (Struhl and Adachi, 2000), these data are consistent with a model in which Dx promotes ectodomain shedding following late endosomal/lysosomal fusion and this is coincident with, or followed by, the degradation of the extracellular domain.

DISCUSSION

A model of Notch activation involving ligand-directed RIP at the cell surface has recently been complicated by several reports showing that Notch endocytosis can precede signal activation (Wilkin et al., 2004; Hori et al., 2004; Moberg et al., 2005; Thompson et al., 2005; Vaccari and Bilder, 2005; Kanwar and Fortini, 2008). Dx is an E3 ubiquitin ligase, which is required for the full activity of Notch in a subset of developmental contexts including the formation of the wing margin (Hori et al., 2004). Dx binds to the Notch intracellular domain and its overexpression promotes

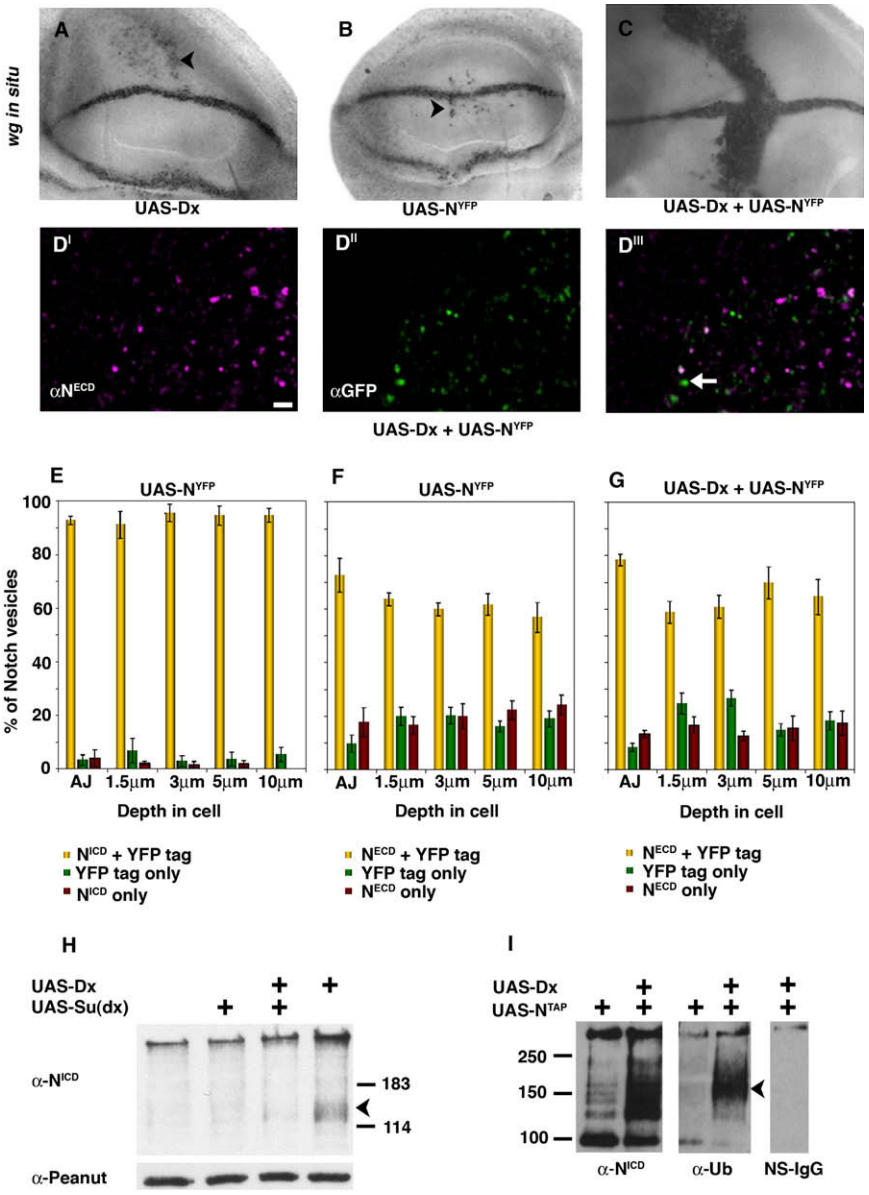

Figure 5. Dx Induces Notch Ectodomain Shedding

(A–C) Overexpression in wing discs of Dx activates the N^{YFP} construct. (Arrowheads in [A and B] indicate weak ectopic *wg*).

(D) Separate vesicular localization of Notch extra- and intracellular domains in a wing disc overexpressing N^{YFP} and Dx. The plane shown is 1.5 μm below the adherens junctions. Arrow in merge (D‴) indicates a vesicle containing only YFP. Scale bar = 2 μm.

(E–G) Quantification of Notch epitope separation in wing discs. Vesicles were scored at the level of the adherens junction and in planes 1.5, 3, 5, and 10 μm more basal. Histograms show relative frequencies of vesicles containing both or single epitopes. Standard error bars are shown. (E) Overexpressed N^{YFP} examined for YFP and N^{ICD} epitope separation. (F and G) Overexpressed N^{YFP} scored for N^{ECD} and YFP epitope separation, (F) in the absence and (G) in the presence of coexpressed Dx.

(H–I) Overexpression of Dx accumulates ubiquitinated, extracellularly truncated Notch fragments. (H) Western blot with anti-N^{ICD} shows that overexpression of Dx increased the intensity of a smear of fragments migrating at 120–140 kDa, which was blocked by coexpressing Su(dx). (I) N^{TAP}, purified from discs either with or without coexpression with Dx, and stained with either anti-N^{ICD}, anti-Ubiquitin (UB), or nonspecific (NS) IgG. Arrowhead marks smear of ubiquitinated Notch present when Dx was coexpressed. Weak nonspecific staining seen with NS is probably uncleaved N^{TAP}. Overexpression in 3rd instar wing discs was performed using Dpp-Gal4 (A–G), or MS1096-Gal4 (H and I).

Notch endocytosis and endocytic-dependent Notch activation, which in the wing results in ectopic margin. We used this phenotype to genetically screen for components required for Dx-induced Notch signaling and identified a number of proteins that comprise the HOPS and AP-3 complexes. In *Drosophila* the proteins encoded by these genes are best known for their role in biogenesis of lysosomal-related pigment granules that contribute to eye color, but they are also involved in the biogenesis of lysosomes, and autophagy (Lloyd et al., 1998; Pulipparacharuvil et al., 2005; Lindmo et al., 2006; Falcon-Perez et al., 2007). Their involvement in activating a developmental signaling pathway has not been demonstrated previously. We used mutations in these components together with manipulations of early/late endosomal trafficking, and immunolocalization studies, to dissect the endocytic Notch activation pathway and to show how the delivery of Notch to the late endosome/lysosome may both activate and downregulate Notch signaling.

A Hierarchy of Endosomal Sorting Signals Control Endocytic Notch Activation and Downregulation

Our results suggest that Dx acts to promote entry of full-length Notch into the endosomal trafficking pathway, and also to direct Notch to the late endosome/lysosome limiting membrane by preventing its sorting into the internal compartments (Figure 7). This would allow the Notch intracellular domain to remain cytoplasmically accessible and available for signaling. We propose that in this location the Notch extracellular domain is subject to proteolytic degradation, being the only part of Notch that would be exposed to the internal lysosomal lumen. The resulting membrane tethered, truncated product would then be a substrate for intramembrane proteolysis by Psn, which is known to be present and active in the limiting lysosomal membrane (Pasternak et al., 2003). This would release the Notch intracellular domain for trafficking to the nucleus and signal activation. Consistent with this model, we found that Dx induced the accumulation of extracellular domain-truncated fragments of Notch in a plane that is 3 μm below the adherens junction. The associated Notch signaling was also shown to be Psn-dependent. Dx promoted the ubiquitination of Notch and it is likely that this covalent modification controls one or both of

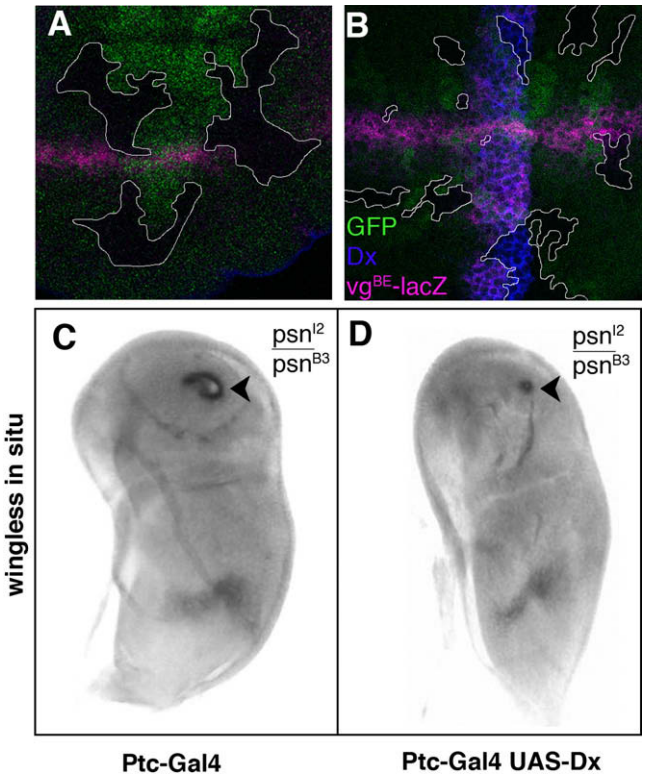

Figure 6. Dx-Induced Notch Signaling Is Dependent on Presenilin

(A and B) *Psn* mutant clones in early-mid third instar wing discs, marked by absence of GFP. (A) In wild-type, Psn deficiency prevents Notch signaling at the D/V boundary, marked by vg^{BE}-lacZ (purple). (B) Ptc-Gal4 driven Dx overexpression (blue) induces ectopic vg^{BE}-lacZ, except in *psn* mutant clones. (C and D) Notch signaling is absent in wing discs of psn^{B3}/psn^{I2} larvae, which have a residual wing pouch, lacking D/V boundary expression of *wg* both in the absence (C) or presence (D) of overexpressed Dx. Arrowheads in (C and D) label Notch-independent *wg* expression outlining the pouch.

the outcomes of Dx activity, as ubiquitination has been associated with many sorting steps in protein trafficking pathways (Mukhopadhyay and Riezman, 2007).

We found that HOPS and AP-3 gene mutations blocked Dx-dependent Notch signal activation. The HOPS complex mediates the progression of early endosomal Rab5 positive vesicles to late endosomal Rab7 positive vesicles (Rink et al., 2005). The AP-3 complex acts as an adaptor in the early endosome and the Golgi, which recognizes sorting signals such as di-leucine motifs and recruits integral membrane proteins for trafficking to the limiting membranes of lysosomes and related organelles (Peden et al., 2004; Theos et al., 2005). It is possible that AP-3 contributes to Notch signaling by ensuring delivery of Notch to the lysosomal limiting membrane, or by allowing the proper lysosomal localization of a membrane protein component that is required for endosomal Notch activation at that location. Our data show that reducing AP-3 function leads to an accumulation of Notch in an enlarged tubular compartment associated with the early endosome, consistent with the former explanation.

Alternative locations for Notch endosomal activation should also be considered however. For example the apparent requirement for HOPS and AP-3 genes for Notch signaling could result from the failure of the degradative removal of nonactivated full-length Notch. In this explanation AP-3 and HOPS mutations may lead to the forced accumulation of full-length Notch in an early endocytic compartment, where it may sequester factors required for the trafficking and Psn-dependent cleavage of ligand-activated Notch. This might explain the dominant-negative effect on endogenous Notch signaling that results from the expression of Dx in an AP-3 or HOPS mutant background. However a number of our results argue against this alternative explanation. First, even though strong early endosomal accumulation of Notch is induced by Rab5 expression, there is no measurable effect on the endogenous Notch signal. Second, the coexpression of Rab7QL with Rab5 activates Notch signaling and this is associated with relocalization of Notch to late endosomal compartments. In addition car^1 mutants suppress the latter ectopic Notch signal, but this does not produce a dominant-negative effect on the endogenous Notch signal. Finally Su(dx) coexpression blocks the Dx-induced signal without causing early endosomal accumulation. Instead it redirects Notch away from the limiting membrane into the center of late endosomal compartments, consistent with our model of endosomal Notch activation.

The developmental role of Dx has been ambiguous because different studies have proposed that it acts either positively or negatively on Notch signaling (Hori et al., 2004; Mukherjee et al., 2005). However our model can now account for these diverse observations. It is possible that combinations of ubiquitin tags on Notch result in a hierarchy of control at different steps in the trafficking pathway that determine a positive or negative outcome on Notch activity. Alternatively Su(dx) might modify the activity of an as yet unknown trafficking regulator. We were unable to detect Su(dx)-dependent Notch ubiquitination using the N^{TAP} pull-down assay (data not shown), however this may be due to deubiquitination of Notch during its transfer to the late endosomal internal lumen (Mukhopadhyay and Riezman, 2007). Further work will be required to understand the biochemical basis of this combinatorial regulation.

Significance of Endosomal Notch Activation for Development and Cancer

Endocytic activation of Notch that occurs ectopically when endosomal sorting is disrupted has previously been shown to be largely independent of DSL ligands (Jaekel and Klein, 2006). We have also shown that signaling induced by overexpression of Dx is independent of DSL ligands (Hori et al., 2004). Here we show that reducing HOPS and AP-3 function does not reduce Notch activation by ectopic ligand expression, but does block the Dx-induced signal, suggesting the existence of two different activation mechanisms. We do not however exclude the possibility that endogenous ligand-initiated signaling can, in part, involve Psn-mediated cleavage in the endosomal pathway. Once ligand promoted ectodomain shedding occurs at the cell surface, the remaining membrane-tethered Notch will become accessible for activation by metalloprotease-mediated S2 and Psn-mediated S3 cleavages. This may occur at the cell surface, but some Notch may enter the endosomal pathway and remain available for activation (Kanwar and Fortini, 2008; Vaccari et al., 2008). It is possible that, following ectodomain shedding, the endosomal entry of membrane-tethered Notch intracellular domain is promoted by Dx. The lack of sensitivity of signaling

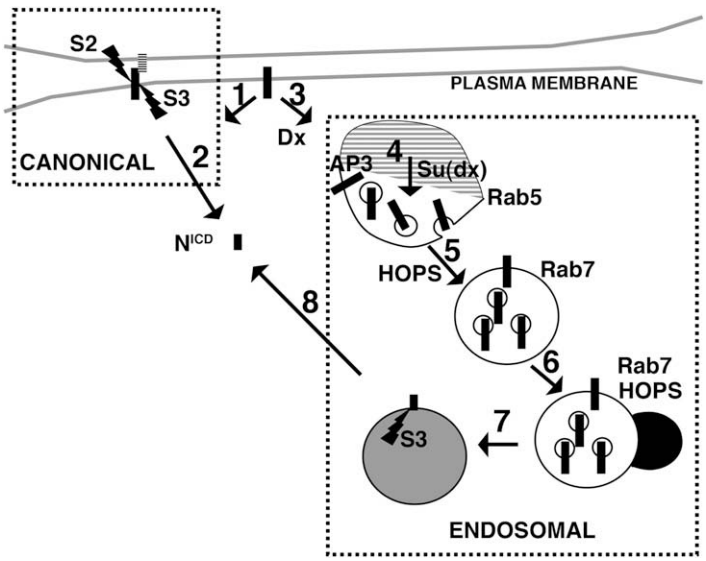

Figure 7. A Model of Notch Signal Regulation through Endocytic Trafficking and Sorting

Full-length Notch (black bar) can be transported to the adherens junctions (1) and be activated by ligands via S2 (metalloprotease-dependent) and S3 (Psn-dependent) proteolytic cleavages (2), which probably occur mainly at the cell surface or within the early endocytic pathway, possibly facilitated through interaction with Dx (not depicted). Alternatively Dx promotes full-length Notch internalization (3), depleting the pool of Notch available for the ligand-dependent pathway. (4) The Dx-internalized Notch is targeted to the late endosome limiting membrane, possibly through interactions with the AP-3 complex. Su(dx) may redirect Dx-internalized Notch to the internal compartments of the multivesicular body. (5) HOPS complex-dependent Rab5-to-Rab7 conversion initiates endosomal maturation to the late endosomes. (6) HOPS complex mediates Rab7-dependent fusion with the lysosome. (7) Notch in internal vesicles is degraded, while Notch that is located at the limiting membrane has its extracellular domain removed by lysosomal proteases. (8) The truncated Notch is targeted for Psn-mediated RIP, thus releasing the N^{ICD}.

induced by ectopically expressed ligands to *car* and *rb* mutations may be because most ligand-induced Psn cleavage of Notch already occurs before Notch is trafficked to the late endosomes. We cannot however rule out a contribution of the late endosomal location in generating a proportion of the endogenous ligand-induced signal. In contrast, when Dx is overexpressed, full-length Notch is removed from the ligand-accessible pool and ectodomain shedding and Notch activation may not then occur until after the AP3- and HOPS-mediated transfer to the late endosomal/lysosomal pool (Figure 7) making Dx-induced signaling critically dependent on this step. At present, however, the amount of signal generated through endocytosis of full-length Notch driven by endogenous Dx cannot be assessed.

The viability of severe or null AP-3 gene mutations (Ooi et al., 1997; Mullins et al., 1999, 2000) and examination of mitotic clones of the null dor^{8} HOPS mutant (Sevrioukov et al., 1999) demonstrates that neither complex is essential for Notch signaling. However, our data suggest that several HOPS and AP-3 components are required to maintain full Notch signaling levels. This may occur through a proportion of ligand-activated, ectodomain shed Notch reaching the late endosome, or through the Dx-driven endocytosis of full-length Notch. We observed that mutations of *lt*, *rb, cm*, and *dx* led to reduction in expression of *sim*, a Notch target gene activated during midline formation. We also observed neurogenic phenotypes, which would be expected from a failure of Notch-mediated lateral inhibition. Interestingly, we also observed mixed phenotypes consisting of both expansion and loss of nervous system. Although the reason for loss of neurons is not yet resolved, it is interesting to speculate whether these variable phenotypes could be accounted for by endocytic trafficking contributing both negatively and positively to Notch activation. In our model, endocytic trafficking will promote the Dx-regulated activation of Notch and also reduce the flux through the canonical DSL ligand-driven pathway by decreasing the ligand accessibility of Notch. The overall contribution of Dx may result from a balance of these opposing effects and this may act to smooth out noise in the Notch signaling levels. If such a smoothing function was not in place then fluctuations might, in some embryos, be amplified by feedback mechanisms beyond acceptable upper or lower thresholds resulting in the mixed phenotypes that we observe. Interestingly the presence of the wild-type Dx/HOPS/AP-3 pathway appears to provide a compensation mechanism that becomes more critical when development proceeds at higher temperatures.

Genetic interactions of *Notch* alleles with loss-of-function mutations in HOPS and AP-3 complex genes indicate that, like Dx, these complexes can contribute to endogenous levels of Notch activity at the wing margin. We did not observe wing margin defects in HOPS or AP-3 mutants in the absence of such genetic interactions, however. Nor did we observe wing margin phenotypes in mitotic clones of *dor8*. It is not clear why *HOPS*, *AP-3*, and *dx* mutants can display similar effects in embryo development but only *dx* displays a wing margin phenotype. It is possible that the latter results, in part, from additional activities of Dx. Alternatively, other factors may partly substitute for AP-3 and HOPS function in some tissues, as has previously been proposed to explain the formation of some pigment granules in null rb^{1} mutants (Mullins et al., 2000). Examples of such redundancy in trafficking routes have also been documented in mammalian cells (Cherqui et al., 2001; Kyttala et al., 2004). On the other hand, *dx* wing phenotypes were enhanced by mutations in other components of the endocytic pathway. This result could be explained if entry of Notch into the endocytic pathway is not completely removed in the absence of *dx*, as has been previously observed (Hori et al., 2004). Interestingly despite both rb^{1} and cm^{1} being null mutations in different AP-3 complex components (Mullins et al., 1999, 2000), the phenotypes of cm^{1} were less severe. Although moderating influences of genetic background cannot be ruled out, other recent work has also shown phenotypic differences between cm^{1} and rb^{1} (Simonsen et al., 2007), suggesting that the developmental requirement of the two genes is not equivalent. Further work will now be required to establish the relative contributions for all the different components of the HOPS and AP-3 complexes and their associated proteins.

Given that the AP-3/HOPS activation pathway is one way in which Notch signaling can acquire ligand-independence, it

should now be considered whether Notch can be ectopically activated by this route in some Notch-dependent tumors. If such tumors are identified, targeting HOPS and AP3 components may preferentially affect the tumor, while sparing normal signaling. Many other proteins have been shown to undergo regulated membrane proteolysis following ectodomain shedding (Landman and Kim, 2004). The finding that the late endosome/lysosome can activate this process for Notch may have implications for understanding the mechanisms of signaling of other developmentally and pathologically relevant membrane receptors.

EXPERIMENTAL PROCEDURES

Drosophila Stocks

A full list of stocks used is provided in the Supplemental Data. All experiments were performed at 25°C on standard *Drosophila* culture medium, unless otherwise stated. Psn^{C1} mutant clones were generated by heat shock-induced (37°C, 30 min) Flp expression in 2nd instar larvae and marked by absence of GFP in early to mid-3rd instar wing imaginal discs. Transgenic expression was performed using the Gal4 system (Brand and Perrimon, 1993). UAS-N^{YFP} was constructed in pUAST by fusing the eYFP (Clontech) sequence in frame with the C terminus of Notch cDNA. Transgenic lines were generated by standard procedures.

In Situ Hybridization

Detection of Notch signaling was by in situ hybridization staining for *wingless* (*wg*) and *sim*, which act as reporters of Notch activity at the dorsal/ventral (D/V) boundary of the wing imaginal disc and embryo midline respectively. In situ hybridization was performed using digoxigenin-labeled antisense cRNA probes and stained with alkaline phosphatase conjugated anti-digoxigenin antibody as previously described (Wilkin et al., 2004).

Immunocytochemistry

For immunofluorescence studies, primary antibodies were: rabbit anti-Arl8 at 1:500 (Hofmann and Munro, 2006); rat anti-Dx (14A) at 1:200 (Busseau et al., 1994); goat anti-GFP at 1:1000 (Abcam); rabbit anti-GFP at 1:5000 (Molecular Probes); mouse anti-Notch extracellular domain (N^{ECD}) (C458.2H); and mouse anti-Notch intracellular domain (N^{ICD}) (C17.9C6), both ascites fluid and used at 1:200 dilution (Developmental Studies Hybridoma Bank [DSHB]); rabbit anti-Rab5 at 1:200 (Wucherpfennig et al., 2003); mouse anti-Wg at 1:20 (4D4, DSHB); anti-ubiquitinated proteins (FK2; used at 1:50; Affinity); rat anti-ELAV at 1:50 (DHSB). Fluorescent secondary antibodies were used at 1:400 and were either CY5-, FITC-, RRX-, or Texas Red-conjugated antisera from Jackson Immunoresearch Laboratories. A standard staining procedure was adopted for processing late third instar larval discs (Wilkin et al., 2004), except for anti-Wg staining when the washes were in PBS + 0.5% Triton X-100 and the initial permeabilization/block was performed using 4% normal donkey serum (Jackson Immunoresearch Laboratories) in PBS + 0.5% Triton X-100. For live disc imaging of lysosomes, discs were stained for 1 hr at room temperature in M3 medium (Sigma) with 50 nM Lysotracker Red DND-99 (Molecular Probes). Embryos were collected by a standard procedure (Ashburner, 1989) and stained using a similar protocol to that used for anti-Wg staining of wing discs except Triton X-100 was 0.3%. Images were captured using a cooled digital camera (Hamamatsu) mounted on a Zeiss Axioskop microscope and processed on an Apple Macintosh computer using Improvision Openlab deconvolution confocal emulation software and Adobe PhotoShop software. Deconvolution was performed using three nearest neighbors from optical sections obtained with a Z spacing of 0.5 μm.

Protein Extracts and Western Blotting for Endogenous Notch Protein

Proteins were extracted from 20 wing discs of each genotype, which were crushed, and solubilized in 40 μl of SDS-PAGE sample buffer. Samples were heated at 95°C for 5 min and separated by 8% SDS-PAGE, western blotted and probed with anti-N^{ICD} used at 1:1000, and horseradish peroxidase conjugated secondary antibody (Sigma) used at 1:1000. Anti-Peanut (DSHB) was used at 1:1000 as a loading control. The blots were visualized using enhanced chemiluminescence (Western Lightning, Perkin Elmer).

In Vivo Assay of Notch Ubiquitination

Expressed N^{TAP} (Veraksa et al., 2005) was purified from protein extracts of late 3rd instar wing discs expressing UAS-N^{TAP}, or UAS-Dx plus UAS-N^{TAP}, under control of the MS1096-Gal4 driver, by affinity chromatography with IgG agarose beads (Sigma). About 30 wing discs per sample, from flies expressing UAS-N^{TAP} or UAS-Dx plus UAS-N^{TAP} were dissected in cold M3 medium (Sigma). The M3 medium was replaced with 200 μl of lysis buffer (10 mM Tris-HCl [pH 7.5], 700 mM NaCl, 0.5% NP40, 2X Complete Protease Inhibitor [Roche]). The discs were crushed with a pestle, briefly vortexed, and then incubated at 37°C for 20 min before the supernatant was removed and added to 20 μl of beads slurry (rabbit IgG agarose beads [Sigma], preblocked with 20% BSA [Sigma] for 1 hr at 4°C, and then equilibrated in the lysis buffer). The mixture was incubated on a rotating wheel at 4°C for 15 min. After incubation, the supernatant was removed following centrifugation and the beads were washed at 4°C, three times for 5 min with lysis buffer, followed by three times for 5 min with cleavage buffer (lysis buffer but without the protease inhibitors). The beads were finally resuspended in 200 μl cleavage buffer and 2 μl of TEV protease (Invitrogen) was added. The sample was incubated on a rotating wheel at room temperature for 2 hr before the supernatant was removed following centrifugation. The supernatant containing the eluted TEV cleaved Notch was precipitated with 10% Trichloroacetic acid. (Note that purified N^{TAP} fragments still have a C-terminal 10 kDa portion of TAP). The pellet was washed by adding 1 ml acetone, air-dried, and then resuspended in 30 μl of standard SDS-PAGE sample buffer. After SDS-PAGE, western blots were probed with anti-N^{ICD} (C17.9C6, Developmental Studies Hybridoma Bank), anti-Ubiquitin at 1:1000 (FK2, Affinity Bioreagents), or nonspecific mouse IgG at 1:1000 (Sigma).

Quantification of Notch Epitope Localization

For each wing disc, immunofluorescence images were acquired for five optical sections corresponding to planes at the apical adherens junction and 1.5 μm, 3 μm, 5 μm, and 10 μm more basal. Vesicles were scored for coincident staining of anti-N^{ECD} and YFP (labeled with anti-GFP), or for either epitope alone, and plotted as a mean frequency derived from six independent wing discs. As a control, discs were also stained for anti-N^{ICD} and anti-GFP and scored as above.

SUPPLEMENTAL DATA

Supplemental Data include Supplemental Experimental Procedures, six figures, one table, and Supplemental References and can be found with this article online at http://www.developmentalcell.com/cgi/content/full/15/5/762/DC1/.

ACKNOWLEDGMENTS

We thank Spyros Artavanis-Tsakonas, Alexey Veraksa, Alfonso Martinez-Arias, Sean Munro, Marcus Gonzalez-Gaitan, Helen Strutt, and Barbara Wakimoto for reagents and *Drosophila* lines, and Sacha Jensen for help to construct the UAS-Ser stock. Several *Drosophila* stocks and antibodies were provided by the Bloomington *Drosophila* Stock Center and the Developmental Studies Hybridoma Bank. We acknowledge financial support from the BBSRC.

Received: May 15, 2007
Revised: July 7, 2008
Accepted: September 3, 2008
Published: November 10, 2008

REFERENCES

Ashburner, M. (1989). *Drosophila*. A Laboratory handbook (Cold Spring Harbor, NY: Cold Spring Harbor Laboratory Press).

Baron, M. (2003). An overview of the Notch signaling pathway. Semin. Cell Dev. Biol. *14*, 113–119.

Brand, A.H., and Perrimon, N. (1993). Targeted gene expression as a means of altering cell fates and generating dominant phenotypes. Development *118*, 401–415.

Bucci, C., Thomsen, P., Nicoziani, P., McCarthy, J., and van Deurs, B. (2000). Rab7: a key to lysosome biogenesis. Mol. Biol. Cell *11*, 467–480.

Busseau, I., Diederich, R.J., Xu, T., and Artavanis-Tsakonas, S. (1994). A member of the Notch group of interacting loci, deltex encodes a cytoplasmic basic protein. Genetics *136*, 585–596.

Cherqui, S., Kalatzis, V., Trugnan, G., and Antignac, C. (2001). The targeting of cystinosin to the lysosomal membrane requires a tyrosine-based signal and a novel sorting motif. J. Biol. Chem. *276*, 13314–13321.

Dupre, S., and Haguenauer-Tsapis, R. (2001). Deubiquitination step in the endocytic pathway of yeast plasma membrane proteins: crucial role of Doa4p ubiquitin isopeptidase. Mol. Cell. Biol. *21*, 4482–4494.

Entchev, E.V., Schwabedissen, A., and Gonzalez-Gaitan, M. (2000). Gradient formation of the TGF-β homolog Dpp. Cell *103*, 981–991.

Falcon-Perez, J.M., Romero-Calderon, R., Brooks, E.S., Krantz, D.E., and Dell'Angelica, E.C. (2007). The *Drosophila* pigmentation gene pink (p) encodes a homologue of human Hermansky-Pudlak syndrome 5 (HPS5). Traffic *8*, 154–168.

Hofmann, I., and Munro, S. (2006). An N-terminally acetylated Arf-like GTPase is localised to lysosomes and affects their motility. J. Cell Sci. *119*, 1494–1503.

Hori, K., Fostier, M., Ito, M., Fuwa, T.J., Go, M.J., Okano, H., Baron, M., and Matsuno, K. (2004). *Drosophila* deltex mediates suppressor of Hairless-independent and late-endosomal activation of Notch signaling. Development *131*, 5527–5537.

Jaekel, R., and Klein, T. (2006). The *Drosophila* Notch inhibitor and tumor suppressor gene lethal (2) giant discs encodes a conserved regulator of endosomal trafficking. Dev. Cell *11*, 655–669.

Kanwar, R., and Fortini, M.E. (2008). The big brain aquaporin is required for endosome maturation and notch receptor trafficking. Cell *133*, 852–863.

Kyttala, A., Ihrke, G., Vesa, J., Schell, M.J., and Luzio, J.P. (2004). Two motifs target Batten disease protein CLN3 to lysosomes in transfected nonneuronal and neuronal cells. Mol. Biol. Cell *15*, 1313–1323.

Lai, E.C. (2004). Notch signaling: control of cell communication and cell fate. Development *131*, 965–973.

Landman, N., and Kim, T.W. (2004). Got RIP? Presenilin-dependent intramembrane proteolysis in growth factor receptor signaling. Cytokine Growth Factor Rev. *15*, 337–351.

Lindmo, K., Simonsen, A., Brech, A., Finley, K., Rusten, T.E., and Stenmark, H. (2006). A dual function for Deep orange in programmed autophagy in the *Drosophila* melanogaster fat body. Exp. Cell Res. *312*, 2018–2027.

Lloyd, V., Ramaswami, M., and Kramer, H. (1998). Not just pretty eyes: *Drosophila* eye-colour mutations and lysosomal delivery. Trends Cell Biol. *8*, 257–259.

Moberg, K.H., Schelble, S., Burdick, S.K., and Hariharan, I.K. (2005). Mutations in erupted, the *Drosophila* ortholog of mammalian tumor susceptibility gene 101, elicit non-cell-autonomous overgrowth. Dev. Cell *9*, 699–710.

Morel, V., and Schweisguth, F. (2000). Repression by suppressor of hairless and activation by Notch are required to define a single row of single-minded expressing cells in the *Drosophila* embryo. Genes Dev. *14*, 377–388.

Mukherjee, A., Veraksa, A., Bauer, A., Rosse, C., Camonis, J., and Artavanis-Tsakonas, S. (2005). Regulation of Notch signaling by non-visual β-arrestin. Nat. Cell Biol. *7*, 1191–1201.

Mukhopadhyay, D., and Riezman, H. (2007). Proteasome-independent functions of ubiquitin in endocytosis and signaling. Science *315*, 201–205.

Mullins, C., Hartnell, L.M., Wassarman, D.A., and Bonifacino, J.S. (1999). Defective expression of the mu3 subunit of the AP-3 adaptor complex in the *Drosophila* pigmentation mutant carmine. Mol. Gen. Genet. *262*, 401–412.

Mullins, C., Hartnell, L.M., and Bonifacino, J.S. (2000). Distinct requirements for the AP-3 adaptor complex in pigment granule and synaptic vesicle biogenesis in *Drosophila melanogaster*. Mol. Gen. Genet. *263*, 1003–1014.

Ooi, C.E., Moreira, J.E., Dell'Angelica, E.C., Poy, G., Wassarman, D.A., and Bonifacino, J.S. (1997). Altered expression of a novel adaptin leads to defective pigment granule biogenesis in the *Drosophila* eye color mutant garnet. EMBO J. *16*, 4508–4518.

Pasternak, S.H., Bagshaw, R.D., Guiral, M., Zhang, S., Ackerley, C.A., Pak, B.J., Callahan, J.W., and Mahuran, D.J. (2003). Presenilin-1, nicastrin, amyloid precursor protein, and γ-secretase activity are co-localized in the lysosomal membrane. J. Biol. Chem. *278*, 26687–26694.

Peden, A.A., Oorschot, V., Hesser, B.A., Austin, C.D., Scheller, R.H., and Klumperman, J. (2004). Localization of the AP-3 adaptor complex defines a novel endosomal exit site for lysosomal membrane proteins. J. Cell Biol. *164*, 1065–1076.

Pfeffer, S. (2003). Membrane domains in the secretory and endocytic pathways. Cell *112*, 507–517.

Pulipparacharuvil, S., Akbar, M.A., Ray, S., Sevrioukov, E.A., Haberman, A.S., Rohrer, J., and Kramer, H. (2005). *Drosophila* Vps16A is required for trafficking to lysosomes and biogenesis of pigment granules. J. Cell Sci. *118*, 3663–3673.

Rink, J., Ghigo, E., Kalaidzidis, Y., and Zerial, M. (2005). Rab conversion as a mechanism of progression from early to late endosomes. Cell *122*, 735–749.

Roy, M., Pear, W.S., and Aster, J.C. (2007). The multifaceted role of Notch in cancer. Curr. Opin. Genet. Dev. *17*, 52–59.

Seals, D.F., Eitzen, G., Margolis, N., Wickner, W.T., and Price, A. (2000). A Ypt/Rab effector complex containing the Sec1 homolog Vps33p is required for homotypic vacuole fusion. Proc. Natl. Acad. Sci. USA *97*, 9402–9407.

Sevrioukov, E.A., He, J.P., Moghrabi, N., Sunio, A., and Krämer, H. (1999). A role for the deep orange and carnation eye color genes in lysosomal delivery in *Drosophila*. Mol. Cell *4*, 479–486.

Simonsen, A., Cumming, R.C., and Finley, K.D. (2007). Linking lysosomal trafficking defects with changes in aging and stress response in *Drosophila*. Autophagy *3*, 499–501.

Struhl, G., and Adachi, A. (2000). Requirements for presenilin-dependent cleavage of notch and other transmembrane proteins. Mol. Cell *6*, 625–636.

Theos, A.C., Tenza, D., Martina, J.A., Hurbain, I., Peden, A.A., Sviderskaya, E.V., and Stewart, A. (2005). Functions of adaptor protein (AP)-3 and AP-1 in tyrosinase sorting from endosomes to melanosomes. Mol. Biol. Cell *16*, 5356–5372.

Thompson, B.J., Mathieu, J., Sung, H.H., Loeser, E., Rorth, P., and Cohen, S.M. (2005). Tumor suppressor properties of the ESCRT-II complex component Vps25 in *Drosophila*. Dev. Cell *9*, 711–720.

Vaccari, T., and Bilder, D. (2005). The *Drosophila* tumor suppressor vps25 prevents nonautonomous overproliferation by regulating notch trafficking. Dev. Cell *9*, 687–698.

Vaccari, T., Lu, H., Kanwar, R., Fortini, M.E., and Bilder, D. (2008). Endosomal entry regulates Notch receptor activation in *Drosophila melanogaster*. J. Cell Biol. *180*, 755–762.

Veraksa, A., Bauer, A., and Artavanis-Tsakonas, S. (2005). Analyzing protein complexes in *Drosophila* with tandem affinity purification-mass spectrometry. Dev. Dyn. *232*, 827–834.

Warner, T.S., Sinclair, D.A., Fitzpatrick, K.A., Singh, M., Devlin, R.H., and Honda, B.M. (1998). The light gene of *Drosophila melanogaster* encodes a homologue of VPS41, a yeast gene involved in cellular-protein trafficking. Genome *41*, 236–243.

Wilkin, M.B., Carbery, A.M., Fostier, M., Aslam, H., Mazaleyrat, S.L., Higgs, J., Myat, A., Evans, D.A., Cornell, M., and Baron, M. (2004). Regulation of notch endosomal sorting and signaling by *Drosophila* Nedd4 family proteins. Curr. Biol. *14*, 2237–2244.

Wucherpfennig, T., Wilsch-Brauninger, M., and Gonzalez-Gaitan, M. (2003). Role of *Drosophila* Rab5 during endosomal trafficking at the synapse and evoked neurotransmitter release. J. Cell Biol. *161*, 609–624.

Wurmser, A.E., Sato, T.K., and Emr, S.D. (2000). New component of the vacuolar class C-Vps complex couples nucleotide exchange on the Ypt7 GTPase to SNARE-dependent docking and fusion. J. Cell Biol. *151*, 551–562.